

Size dependence of ordering in FePt nanoparticles

Y. K. Takahashi,^{a)} T. Koyama, M. Ohnuma, T. Ohkubo, and K. Hono

National Institute for Materials Science (NIMS), 1-2-1 Sengen, Tsukuba 305-0047, Japan

(Received 11 September 2003; accepted 1 December 2003)

We have investigated the size effect of $A1 \rightarrow L1_0$ ordering of FePt nanoparticles in FePt–Al₂O₃ granular and FePt/SiO₂ particulate films by transmission electron microscopy (TEM). The TEM results have shown convincingly that ordering does not progress when the particle size has a diameter of less than 4 nm. Calculation of the order parameter profile from the surface to the volume of the FePt nanoparticles based on diffuse-interface theory justified the experimentally observed size dependence of the ordering. The transition length from disorder to order depends on the interfacial energy, hence the critical particle size of ordering should vary depending on the type of matrix and substrate. © 2004 American Institute of Physics. [DOI: 10.1063/1.1643187]

I. INTRODUCTION

Dispersoids of FePt nanoparticles attract great research interest for possible application to ultrahigh density magnetic recording media. In recording media with areal density of 1 Tbit/in.², the size of ferromagnetic particles is less than 10 nm in diameter. Since the $L1_0$ FePt phase has large magnetocrystalline anisotropy (7×10^7 erg/cc),¹ $L1_0$ FePt particles are thermally stable even when they are of nanometer dimensions. For this reason, many attempts have been made to fabricate magnetically decoupled FePt nanogranular films,^{2–6} in which the nanosized FePt particles are dispersed in the nonmagnetic oxide matrix.

When films are fabricated by vapor deposition or sputtering processes, FePt particles have a disordered face-centered-cubic (fcc) structure even though the thermodynamic ordering temperature of the $L1_0$ FePt phase is 1573 K. This is because the particles do not pass through the order-disorder temperature during growth from vapor. Hence, high temperature *ex situ* annealing above 773 K is necessary to transform the disordered fcc phase into the $L1_0$ ordered phase after the fabrication of films.^{2–6} However, grain growth occurs concurrently with ordering at this elevated temperature and results in coalescence of the particles and magnetic coupling of the ferromagnetic particles.^{2–6} Ordering to the $L1_0$ structure without coarsening and coalescence of the nanoparticles is required to produce FePt nanogranular films that are suitable for recording media application. However, to the best of the authors' knowledge, ordered FePt particles are observed only after the coalescence of nanoparticles in all previous investigations.^{2,4–10}

To increase the areal density in magnetic recording, the size of ferromagnetic particles is becoming increasingly smaller. The $L1_0$ FePt phase attracts much attention because of its small critical size for superparamagnetism of about 3 nm at room temperature. However, recent investigations reported that FePt particles that are smaller than a certain critical size do not order into the $L1_0$ structure by annealing.^{11,12} In our previous study, we explained these experimental observations based on depression of the thermodynamical or-

dering temperature in nanoparticles as a result of increased surface (or interfacial) energy with respect to the volume free energy.¹¹ In this work, we establish the size dependence of the ordering of FePt nanoparticles by further experiments and give a reasonable interpretation of the experimental results based on calculation of the long-range order parameter profiles based on diffuse-interface theory.^{13,14}

II. EXPERIMENT

Sputter-deposited FePt–Al₂O₃ granular films and FePt particulate films were annealed in this study to examine the size dependence of ordering. The FePt–Al₂O₃ granular films were fabricated by annealing multilayers of FePt 0.5 nm/Al₂O₃ x nm films that were prepared by alternate sputtering of FePt and Al₂O₃ layers, where x was 0.5 and 2 nm. The FePt layer was deposited by dc magnetron sputtering Fe and Pt targets, and the Al₂O₃ layer was deposited by rf magnetron sputtering an Al₂O₃ target at room temperature. The multilayer films were annealed at 873 K for 1, 54, and 192 h. The FePt particulate films were fabricated on an amorphous SiO₂ substrate heated at 973 K. Under these conditions, films grow in Volmer–Weber growth mode, and films that are less than 20 nm are comprised of island-like FePt nanoparticles on the substrate.¹⁵ To change the particle size, the film thickness was changed from 0.5 to 20 nm. The base pressure of the sputtering chamber was better than 6.0×10^{-7} Pa. Thermally oxidized Si wafers were used as substrates, on which the amorphous SiO₂ layer was present. The Ar gas pressure was maintained at 0.1 Pa during film growth.

The structure of the films was examined by a standard x-ray diffractometer (XRD) using Cu $K\alpha$ radiation. The microstructure of the films was examined by a Philips CM200 transmission electron microscope (TEM) and JEOL JEM-4000EX high resolution electron microscope (HREM). The composition of the FePt particles was estimated by energy dispersive x-ray spectroscopy (EDXS) on a TEM. The composition of the FePt particles in this experiment was about Fe₅₀Pt₅₀. The particle size was determined by small-angle x-ray scattering (SAXS) using a Rigaku PSAXS-3S apparatus with pinhole collimation and a Mo target. The particle diameter was estimated by sphere approximation from the

^{a)}Corresponding author; electronic mail: takahashi.yukiko@nims.go.jp

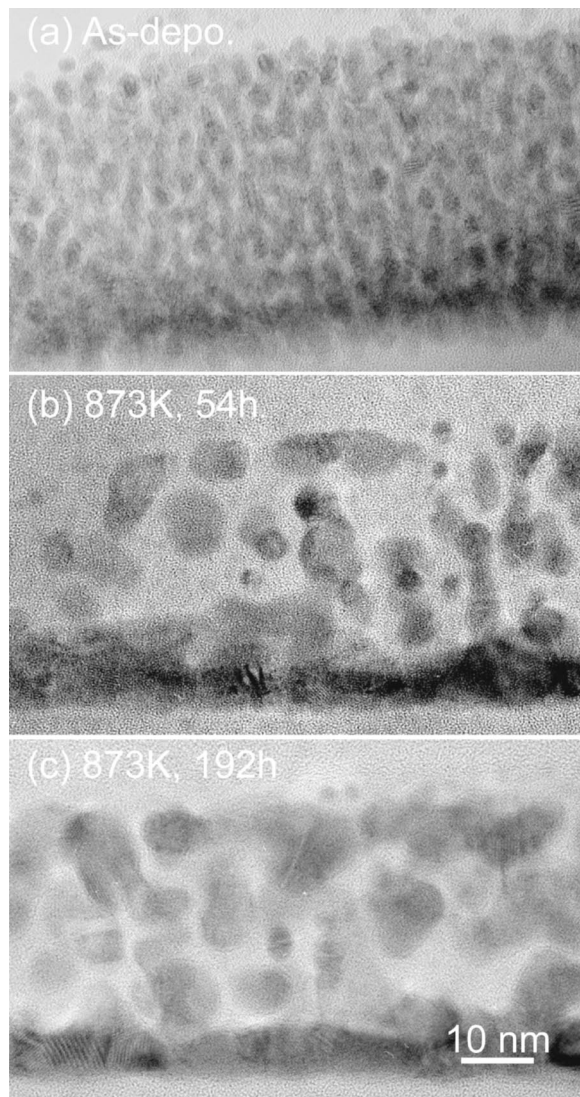


FIG. 1. HREM images of the (a) as-deposited FePt 0.5 nm/Al₂O₃ 0.5 nm multilayer film and of those annealed at 873 K for (b) 54 and (c) 192 h.

radius of gyration, R_g , which was obtained by a Guinier plot of SAXS profiles using $d=2R_g\sqrt{5/3}$. The magnetization curves of the films were measured by a superconducting quantum interference device (SQUID) magnetometer.

III. RESULTS

A. FePt–Al₂O₃ granular film

Figure 1 shows cross-sectional HREM images of a FePt 0.5 nm/Al₂O₃ 0.5 nm multilayer film and of those annealed at 873 K for 54 and 192 h. In the as-deposited film, the film has a granular structure, not a multilayer structure. The particle size of the as-deposited sample determined by SAXS is about 4 nm. Coarsening and coalescence occurred in the film after annealing at 873 K for 54 and 192 h. The particle size increased to about 8 nm in both cases. Figure 2 shows cross-sectional HREM images of a FePt 0.5 nm/Al₂O₃ 2 nm multilayer film and those annealed at 873 K for 54 and 192 h. Although the multilayer structure of FePt and Al₂O₃ is clearly observed in the as-deposited film, the FePt particles do not form a continuous layer but instead are isolated by the

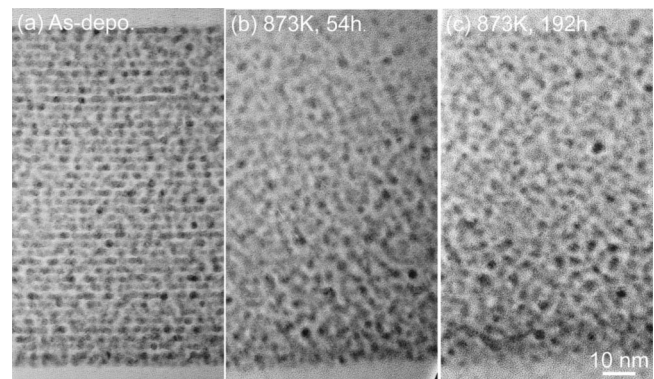


FIG. 2. HREM images of the (a) as-deposited FePt 0.5 nm/Al₂O₃ 2 nm multilayer film and of those annealed at 873 K for (b) 54 and (c) 192 h.

Al₂O₃ matrix. The average particle size is about 3.5 nm. After annealing at 873 K for 54 and 192 h, the multilayer structure breaks and becomes an isotropic granular structure. However, in contrast to Fig. 1, the particle size does not increase. Figure 3 shows plan-view TEM bright field images of the FePt 0.5 nm/Al₂O₃ 0.5 nm and FePt 0.5 nm/Al₂O₃ 2 nm multilayer films annealed at 873 K for 1, 54, and 192 h. Corresponding selected area electron diffraction (SAED) patterns are also shown. The SAED patterns of the annealed FePt 0.5 nm/Al₂O₃ 0.5 nm multilayer films [Figs. 3(a)–3(c)] show that the FePt particles embedded in the amorphous Al₂O₃ are ordered to the $L1_0$ structure. On the other hand, the SAED patterns of the annealed FePt 0.5 nm/Al₂O₃ 2 nm multilayer films [Figs. 3(d)–3(f)] show that the FePt particles are in a disordered state. In the FePt 0.5 nm/Al₂O₃ 0.5 nm multilayer film, the particle size is about 5.9 nm after annealing at 873 K for 1 h, about 7.8 nm after annealing for 54 h, and about 8.1 nm after annealing for 192 h while the particle size of the FePt 0.5 nm/Al₂O₃ 2 nm multilayer film is about 3.5 nm even after annealing for up to 192 h. The particle size is almost the same regardless of the annealing time. The particle size increases by annealing in the sample containing a high volume fraction of FePt, but the particles do not coarsen in the film with a low volume fraction of FePt.

To evaluate the degree of order, s^2 , the integrated intensity of the SAED patterns was measured by a slow scan charge coupled device (CCD) camera. s^2 is defined as

$$s^2 = \frac{\{I_{(110)}/I_{(111)}\}_{\text{measured}}}{\{I_{(110)}/I_{(111)}\}_{s=1}}. \quad (1)$$

Here, $I_{(hkl)}$ is the integrated intensity of the (hkl) diffraction ring. We confirmed that FePt particles are randomly oriented from the integrated intensity ratio. Figure 4 shows the change of s^2 as a function of the particles size, where the particle size is measured by SAXS. s^2 increases with an increase in the particle size. The continuous film annealed at 873 K for 1 h shows $s^2=1$. s^2 is zero for particles smaller than 3.5 nm. This means that the FePt particle that is smaller than 3.5 nm does not order by annealing at 873 K.

Figure 5 shows magnetization curves of the as-deposited and annealed FePt 0.5 nm/Al₂O₃ 0.5 nm and FePt 0.5 nm/Al₂O₃ 2 nm multilayer films. The FePt 0.5 nm/Al₂O₃ 0.5 nm multilayer film shows magnetically soft hysteresis in the as-

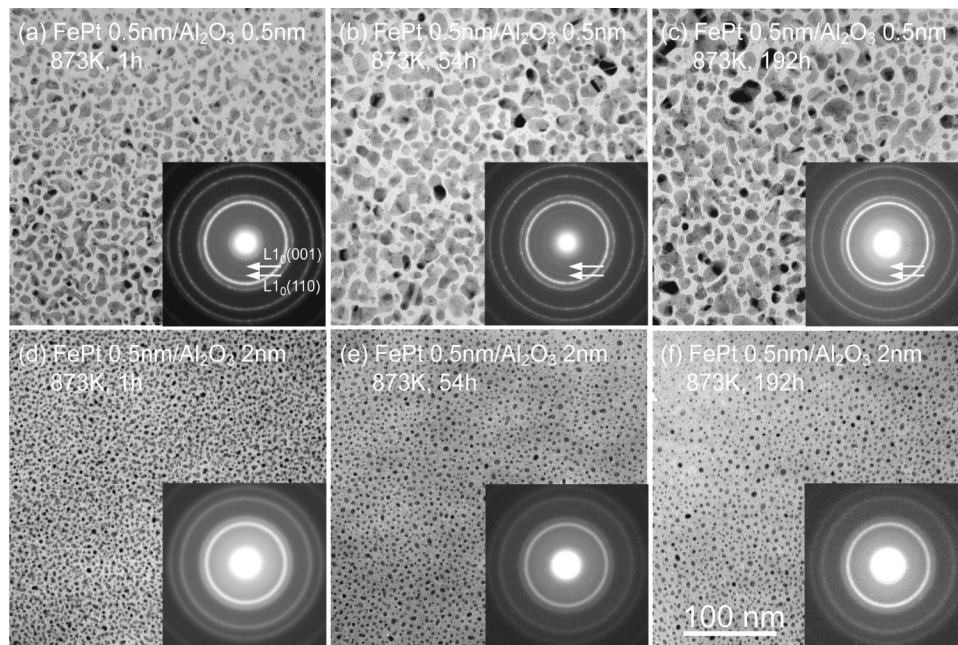


FIG. 3. TEM images and electron diffraction patterns of FePt 0.5 nm/Al₂O₃ 0.5 nm multilayer film annealed at 873 K for (a) 1, (b) 54, and (c) 192 h and of FePt 0.5 nm/Al₂O₃ 2 nm multilayer film annealed at 873 K for (d) 1, (e) 54, and (f) 192 h.

deposited state. After annealing at 873 K, the coercivity increased with an increase in the annealing time. This increase of the coercivity is due to the increase of s^2 . On the other hand, the FePt 0.5 nm/Al₂O₃ 2 nm multilayer film shows superparamagnetism even after annealing. This is because ordering did not progress in these films even after annealing at 873 K for 192 h. Since coarsening and coalescence of the particles do not occur by annealing in this film, the films show superparamagnetism.

B. FePt particulate film

Figure 6 shows XRD patterns of FePt particulate films deposited on an amorphous SiO₂ layer at 973 K. The numbers indicated above the XRD patterns are the nominal thicknesses of the films that are estimated from the sputtering rate. The sharp peaks observed at around $2\theta=33^\circ$ and 69° are from the Si substrate. The XRD patterns of the films with a thickness of more than 3 nm exhibit a (001) superlattice reflection at around $2\theta=24^\circ$ with preferred orientation of (001). No diffraction is observed in the films that are thinner

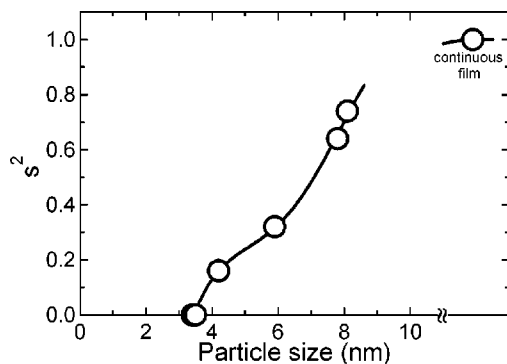


FIG. 4. Change in the degree of order, s^2 , as a function of the particle size in the Al₂O₃ matrix.

than 2 nm because of the small volume of diffraction. Figure 7 shows the TEM bright field images and SAED patterns of these films. Superlattice diffraction rings are clearly observed in the SAED patterns: they are indicated by arrows in the films with thickness of more than 2 nm. On the other hand, only fundamental diffraction rings are observed in the SAED patterns in the films that are thinner than 1 nm. The bright field images show that all the films are composed of isolated FePt particles. The particle size increases with the thickness of the films because of coarsening and coalescence of the particles during film growth. Twins are commonly observed in the FePt particles in the films with thickness of more than 2 nm. These twins are introduced to relieve the strain caused

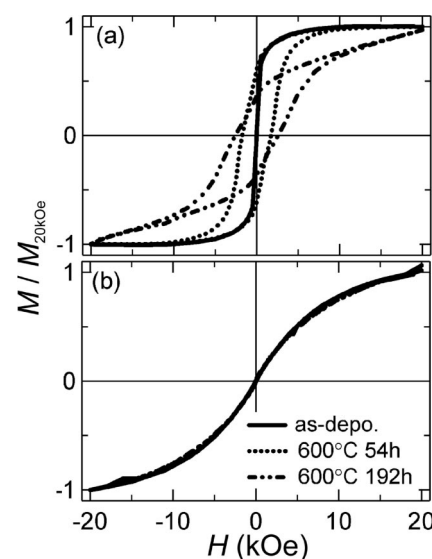


FIG. 5. In-plane hysteresis loops for (a) FePt 0.5 nm/Al₂O₃ 0.5 nm multilayer film and (b) FePt 0.5 nm/Al₂O₃ 2 nm multilayer film after annealing at 873 K for various times.

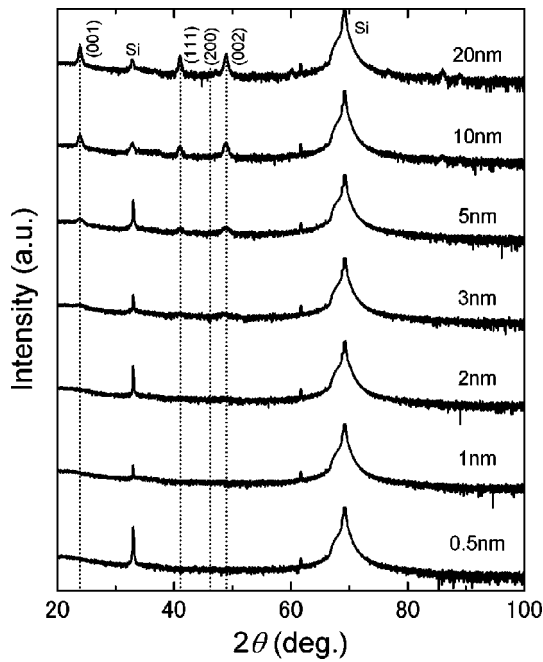


FIG. 6. X-ray diffraction patterns for various thicknesses of the FePt films deposited on the heated substrate at 973 K.

by distortion as a result of the transformation from fcc to face-centered-tetragonal (fct). However, no transformation twins are observed in the 1 nm thick film, indicating that the particles in this film do not order to the $L1_0$ structure.

Figure 8 shows the change of s^2 as a function of the particle size. The particle size of the films with thickness of more than 2 nm was determined by SAXS. The particle size of the 0.5 and 1 nm thick films was determined by TEM, because the intensity of SAXS profiles was too weak to analyze. s^2 was evaluated from the ratio of (001) and (002) integrated intensities of the XRD pattern for the films with

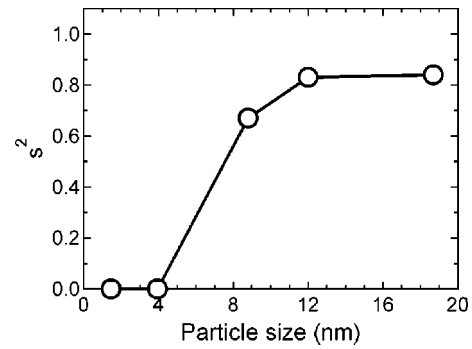


FIG. 8. Change in the degree of order, s^2 , as a function of the particle size of the FePt particulate film.

thickness of more than 3 nm. For films thinner than 2 nm, s^2 was determined from the integrated intensities of the SAED patterns because the XRD intensities were too weak. As shown in Fig. 8, s^2 increases with an increase in the particle size. When the particle size is smaller than 4 nm, s^2 is zero. This means that the FePt particle which is smaller than 4 nm does not order at 973 K on the amorphous SiO_2 substrate.

Figure 9 shows magnetization curves of FePt particulate films with various thicknesses. The 1 nm thick film shows a Langevin type curve, suggesting that the nanoparticles are magnetically isolated and thermally unstable, that is, the film is superparamagnetic. The 2 nm thick film shows curves of a combination of superparamagnetism and hard magnetism. From the TEM observation result [Fig. 7(c)], a size distribution can be seen in the FePt particles. Since the particles smaller than the critical size will be thermally unstable, the magnetization curve contains both ferromagnetic and superparamagnetic components. Another possible reason for the superparamagnetic component is the low s^2 of the particles. Because s^2 is about 0.7, the magnetocrystalline anisotropy

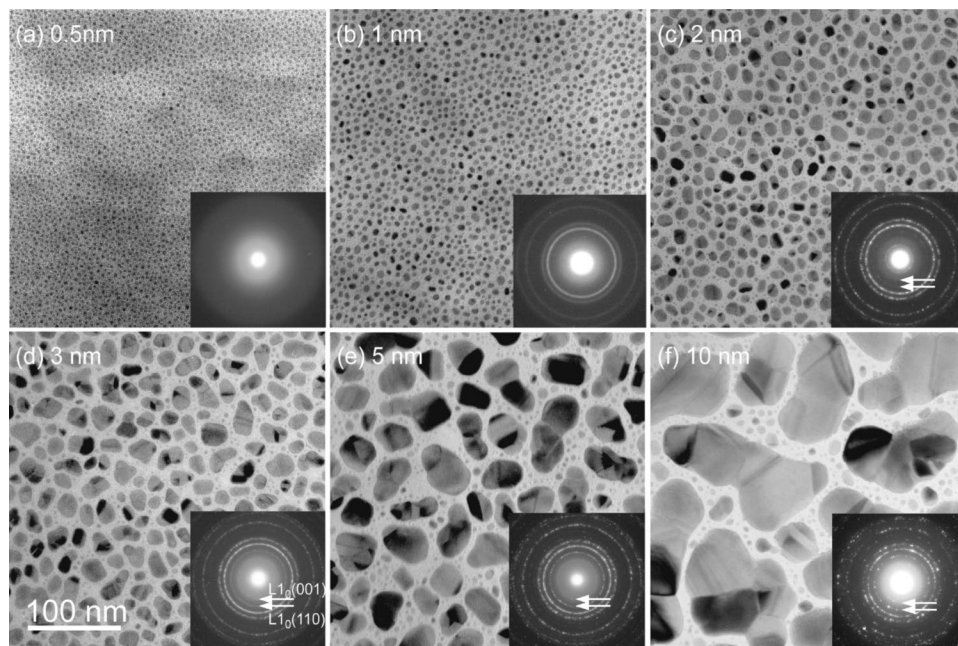


FIG. 7. TEM images and electron diffraction patterns of the various thicknesses of the FePt films deposited on the heated substrate at 973 K.

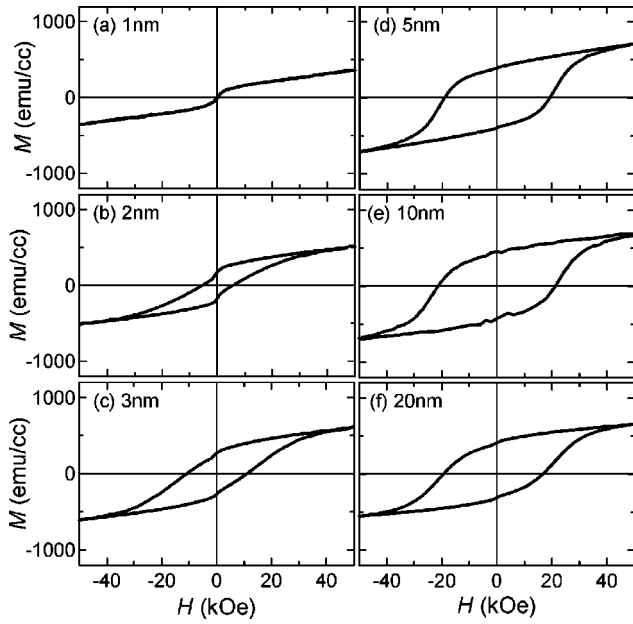


FIG. 9. In-plane hysteresis loops for various thicknesses of the FePt particulate film.

would be lower than that of the perfectly ordered FePt. Therefore, the critical particle size for superparamagnetism would be large. With an increase in film thickness, the number of superparamagnetic particles decreases and the coercivity increases. The magnetization of the ordered FePt does not saturate even at a magnetic field of 55 kOe because of the random orientation of the FePt particles with very large magnetocrystalline anisotropy.

IV. DISCUSSION

The present experimental results clearly show that there is a critical size for the ordering of FePt particles, below which the fcc FePt particles do not order by annealing at elevated temperature. This means that there will be a limit in the recording density that can be achieved using $L1_0$ FePt particles. Here, we justify the experimental results of the size dependence of the $A1 \rightarrow L1_0$ ordering in FePt nanoparticles. The calculation is based on diffuse-interface theory originally proposed by Cahn and Hilliard¹³ and modified by Poduri and Chen.¹⁴ Since we assume that a FePt nanoparticle has a homogeneous composition, c_0 , the total free energy, depending on the order–disorder transition, F , is given by

$$F = \int [f(s, c_0) + \kappa_s |\nabla s|^2] d^3x, \quad (2)$$

where $f(s, c_0)$ is the local free energy density defined as a function of the long-range order parameter s and composition c_0 . Completely disordered fcc and $L1_0$ ordered states are represented by $s=0$ and ± 1 , respectively. The value of the order parameter commonly changes with the temperature and composition. The order parameter described above is normalized by the value of the equilibrium of the order parameter at a given temperature and composition. κ_s is the gradient energy coefficient of order parameter s . The increase

TABLE I. Numerical values used for calculation.

	0.450	0.500
c_0	0.450	0.500
T/K	923	873
$W(c_0, T)/J \text{ mol}^{-1}$	2.242×10^3	3.820×10^3
$\Delta x/m$	1.38×10^{-9}	1.38×10^{-9}
$\kappa_s/m^2 J \text{ mol}^{-1}$	1.07×10^{-15}	1.07×10^{-15}

in total free energy that arises from long-range order parameter fluctuation in the particle is then given by

$$\Delta F = \int [\Delta f(s, c_0) + \kappa_s |\nabla s|^2] d^3x, \quad (3)$$

where we define the function $\Delta f(s, c_0)$ as

$$\begin{aligned} \Delta f(s, c_0) &= f(s, c_0) - f(0, c_0) \\ &= W(c_0, T)(1+s)^2(1-s)^2. \end{aligned} \quad (4)$$

Because $\Delta f(1, c_0) - \Delta f(0, c_0) = -W(c_0, T)$, $W(c_0, T)$ is the driving force for ordering that is evaluated from CALPHAD type thermodynamic data for the Fe–Pt binary alloy system estimated by Fredriksson and Sundman.¹⁶ The gradient energy coefficient is calculated by

$$\kappa_s = \frac{1}{4} W(c_0, T) (\Delta x)^2, \quad (5)$$

where Δx is the width of the antiphase boundary (APB) in the $L1_0$ ordered phase. Equation (5) is obtained easily from analytical solution of the one-dimensional stable order parameter profile across an APB. To determine the value of κ_s , we used the experimental data of Δx at 923 K.² The numerical values used for the calculation are summarized in Table I.

If we assume that the system is isotropic, i.e., κ_s is constant, and the shape of the FePt nanoparticle has spherical symmetry, the stable long-range order parameter profile should satisfy the Euler equation in spherical coordinates,

$$2\kappa_s \frac{d^2s}{dr^2} + \frac{4\kappa_s}{r} \frac{ds}{dr} = \frac{\partial \Delta f}{\partial s}, \quad (6)$$

with the boundary conditions,

$$\frac{ds}{dr} = 0 \quad \text{at } r=0$$

and

$$s=0 \quad \text{at } r=d/2,$$

where d is the diameter of the FePt particle. This second-order differential equation is solved numerically for various values of d .

Figure 10(a) shows the calculation result of the stable order parameter profiles with different particle size, d . When particle size d is larger than about 5 nm, the shape of the order parameter profile at the surface region remains almost constant. If particle size d is smaller than 5 nm, the order parameter value at the center of the profile goes down as the size decreases and the global shape of the profile becomes smooth. When the particle size is less than about 2 nm, the ordered state within the grain becomes unstable, which means that the order–disorder transition depends on the particle size and a critical size for ordering should exist. A

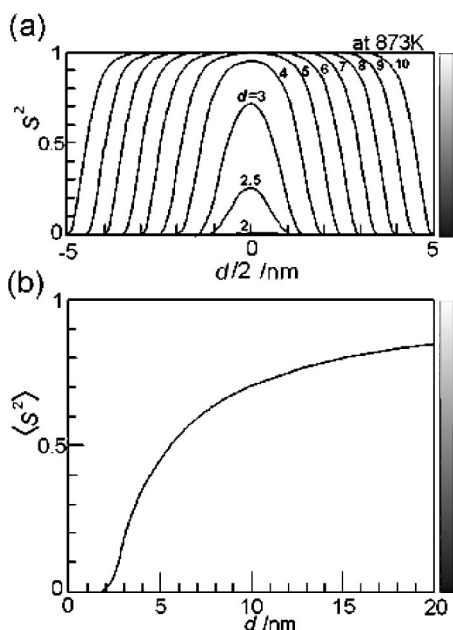


FIG. 10. (a) Calculation results for the stable order parameter profile with different particle sizes, d , at 873 K. The numerical values shown indicate particle size d . (b) Particle size dependence of the average value of the order parameter, $\langle s^2 \rangle$.

change of the average value of the order parameter in the particle with respect to the particle size is shown in Fig. 10(b). The size dependence of the order parameter resembles experimentally measured ordered parameters as a function of the particle size (Figs. 4 and 8). By extrapolating the curve in Fig. 10(b) to the abscissa, we obtain the critical size for ordering to be about 2 nm. On the other hand, the experimentally determined critical size for ordering is about 4 nm. Since the gray scale on the right-hand side of Figs. 10(a) and 10(b) is proportional to the square of the order parameter, the whiteness in the gray scale corresponds to the intensity of the ordered reflection spot in the diffraction pattern. When the particle size is less than 3 nm, the ordering spot in the diffraction pattern is quite weak. Ordering was confirmed in the experiment after the particle size became larger than 5 nm. Thus, the experimental critical size for ordering is around 4 nm, which is in relatively good agreement with the calculation result.

From these experimental and calculation results, we conclude that 4 nm FePt particles in the Al_2O_3 matrix and that deposited on a heated SiO_2 substrate at 973 K do not order. However, $L1_0$ ordering of FePt particles with diameter of less than 4 nm was previously reported.¹⁷ The size dependence of ordering appears because the interface between the FePt and the matrix material is disordered, so the ordering in the nanosized particle becomes unstable when the fraction of the interface increases. Hence, the critical size will vary depending on the interfacial energy. The above report of ordering in a 4 nm particle is probably due to the low interfacial energy of the sample. In this work, no significant difference was observed in the critical size of ordering between the FePt/ Al_2O_3 granular film and the FePt/amorphous- SiO_2 particulate film. This indicates that the total interfacial energy of these two systems as similar.

In our previous paper, we reported that the size dependence of $L1_0$ ordering of FePt particles is due to the depression of thermodynamical order-disorder temperature (T_c) when the particle size become less than 10 nm. The present calculation result based on diffuse-interface theory does not contradict our previous conclusions. In this work, the critical size was calculated for annealing temperature of 873 K. Since $W(c_0, T)$ varies, depending on the temperature, the critical size should be larger at higher temperature. In other words, 873 K is the T_c for the FePt particle with diameter of 4 nm. So the present explanation for the size dependence of $L1_0$ ordering of the FePt particle is just a different expression of the T_c depression as a function of the particle size.

V. SUMMARY

To clarify the size dependence of the $L1_0$ ordering of FePt particles, FePt/ Al_2O_3 granular films and FePt/ SiO_2 particulate films were fabricated by the sputtering technique. TEM observation results convincingly showed that fcc FePt particles with diameter of less than 4 nm do not order to the $L1_0$ structure even if they are annealed at 873 K for a prolonged period of time. The size effect of ordering was reproduced by the order parameter calculation based on diffuse-interface theory. The size effect of ordering appears when the surface volume fraction becomes dominant in nanosized particles, because the interface between the particle and the matrix is disordered. The transition length from disorder to order depends on the interfacial energy, thus the critical size of ordering varies, depending on the type of substrate and matrix.

ACKNOWLEDGMENTS

This work was partly supported by the Special Coordination Funds for Promoting Science and Technology for “Nanohetero Metallic Materials” of the Ministry of Education, Culture, Sports, Science and Technology. One of the authors (Y.K.T.) acknowledges the Japan Science Promotion Society for a fellowship.

¹O. A. Ivanov, L. V. Solina, V. A. Demshina, and L. M. Maget, *Phys. Met. Metallogr.* **35**, 81 (1973).

²M. Watanabe, T. Masumoto, D. H. Ping, and K. Hono, *Appl. Phys. Lett.* **76**, 3971 (2000).

³M. L. Yan, H. Zeng, N. Powers, and D. J. Sellmyer, *J. Appl. Phys.* **91**, 8471 (2002).

⁴H. Zeng, S. Sun, T. S. Vedantam, J. P. Liu, and Z. L. Wang, *Appl. Phys. Lett.* **80**, 2583 (2002).

⁵P. C. Kuo, S. C. Chen, Y. D. Yao, A. C. Sun, and C. C. Chiang, *J. Appl. Phys.* **91**, 8638 (2002).

⁶T. Saito, O. Kitakami, and Y. Shimada, *J. Magn. Magn. Mater.* **239**, 310 (2002).

⁷Y. K. Takahashi, M. Ohnuma, and K. Hono, *J. Magn. Magn. Mater.* **246**, 259 (2002).

⁸Y. K. Takahashi, M. Ohnuma, and K. Hono, *J. Appl. Phys.* **93**, 7580 (2003).

⁹Y. Ding, S. Yamamuro, D. Farrel, and S. A. Majetich, *J. Appl. Phys.* **93**, 7411 (2003).

¹⁰Y. Zhang, J. Wan, M. J. Bonder, G. C. Hadjipanayis, and D. Weller, *J. Appl. Phys.* **93**, 7175 (2003).

¹¹Y. K. Takahashi, T. Ohkubo, M. Ohnuma, and K. Hono, *J. Appl. Phys.* **93**, 7166 (2003).

¹²B. Stal *et al.*, *Phys. Rev. B* **67**, 014422 (2003).

- ¹³J. W. Cahn and J. E. Hilliard, *J. Chem. Phys.* **31**, 688 (1959).
- ¹⁴R. Poduri and L.-Q. Chen, *Acta Mater.* **44**, 4253 (1996).
- ¹⁵T. Shima, K. Takanashi, Y. K. Takahashi, and K. Hono, *Appl. Phys. Lett.* **81**, 1050 (2002).
- ¹⁶P. Fredriksson and B. Sundman, *CALPHAD: Comput. Coupling Phase Diagrams Thermochem.* **25**, 535 (2001).
- ¹⁷K. Sato, M. Fujiyoshi, M. Ishimaru, and Y. Hirotsu, *Scr. Mater.* **48**, 921 (2003).